

Numerical Study on Flexural Response of Cement Mortars Fortified with Sustainable Graphene Derivative

Mohammad Zuaiteer^{1,2}, Tae-Yeon Kim^{1,2}, Rashid K. Abu Al-Rub², and Fawzi Banat³

¹ Department of Civil and Environmental Engineering, Khalifa University of Science and Technology, Abu Dhabi, 127788, United Arab Emirates
100063733@ku.ac.ae; taeyeon.kim@ku.ac.ae

² Advanced Digital & Additive Manufacturing Centre, Khalifa University of Science and Technology, Abu Dhabi, 127788, United Arab Emirates

³ Department of Chemical and Petroleum Engineering, Khalifa University of Science and Technology, Abu Dhabi, 127788, United Arab Emirates

Abstract - This study aims to predict the flexural response through a 3D non-linear finite element model of plain and modified cement mortar incorporating a sustainable graphene derivative, denoted as D-GSH, synthesized from dune sand and date syrup. The addition of D-GSH in cement mortars was considered by dune sand replacement. Preliminary experimental compressive strength and modulus of elasticity yielded 53 and 45% enhancements upon the addition of 0.3% D-GSH, as a replacement of dune sand. ABAQUS software was employed to simulate a three-point load test on mortar prism specimens, encompassing both tensile cracking and compressive crushing mechanisms. Numerical simulation of three-point bending tests revealed a notable 27% increase in peak load and a 16% larger mid-span deflection upon the addition of 0.3% D-GSH, replaced by dune sand in cement mortars, demonstrating improved resistance and deformability.

Keywords: sustainable synthesized graphene, graphene-coated sand, flexural strength, finite element.

1. Introduction

For several decades, concrete has been widely favored in the construction industry for its exceptional resistance to compressive loading. However, its use is constrained by inherent limitations such as brittleness, poor tensile and flexural strengths, and susceptibility to cracking [1], [2], [16]. To address these challenges, researchers have explored various avenues, including the incorporation of fibers like steel, polypropylene, carbon, and glass, to enhance ductility and reduce crack widths [3], [4]. However, the addition of fibers has limitations, as it does not effectively address the formation and initiation of pores and cracks at the nanoscale and may increase the density of the composite. To overcome these issues, there has been a growing interest in introducing nanomaterials into the cement matrix to produce stronger and more durable cement composites [5].

Nanomaterials offer benefits such as filling nano-scale pores, limiting crack initiation and progression, reducing crack widths through a bridging effect, strengthening the interfacial transition zone (ITZ), and promoting a refined microstructure through enhanced hydration reactions [6]. The addition of small quantities of nanomaterials can achieve these improvements without significantly increasing the weight of the composite [7]. Graphene has shown promise in accelerating cement hydration, producing denser cement, and influencing the mechanical behavior of cementitious composites [8]. Different forms of graphene, including graphene nanoplatelets, graphene oxide, and reduced graphene oxide, have been well investigated in the literature [9]. However, other sustainable forms of graphene were never introduced nor investigated in cementitious composites. In this study, the aim is to investigate the effect of sustainable synthesized graphene from date syrup and desert sand particles, referred to herein as date-based graphene sand hybrid (D-GSH) [10]. D-GSH is chosen for its sustainability, cost-effectiveness, and abundance in the UAE and nearby regions.

Building upon this foundation, the current investigation delves into exploring the impact of D-GSH addition in cement mortars on the overall flexural behavior through numerical simulation. This exploration is conducted through finite element (FE) modeling, employing ABAQUS software.

2. Material Properties

Table 1 outlines the proportions of the investigated mixes, with plain cement mortar serving as a benchmark to demonstrate the impact of 0.3% D-GSH addition, replaced by dune sand. The 28-day compressive strength and modulus of

elasticity were experimentally determined according to ASTM C109 [11] and ASTM C580-02 [12]. The plain and D-GSH cement mortars exhibited 28-day compressive strengths of 30 and 46 MPa, respectively, with corresponding 28-day moduli of elasticity of 1 and 1.45 GPa and hardened densities of 2052 and 2098 kg/m³. These values were incorporated into ABAQUS for numerical simulation. The simulation considered two primary failure mechanisms: tensile cracking and compressive crushing of cement mortar elements, as illustrated in Figure 1(a-b). The cement mortars were simulated as elastoplastic materials, with plastic flow potential defined by a dilation angle of 40 degrees. The equibiaxial strength to compressive strength ratio (f_{b0}/f_{c0}) was maintained at 1.16, as recommended for cement mortars [13], [14]. Other plasticity parameters such as eccentricity, K constant, and viscosity were taken as 0.1, 0.667, and 0.001, respectively. In the three-point bending test model, stainless steel plates and supports with Young's modulus of 21000 MPa and Poisson's ratio of 0.35 were considered.

Table 1: Mixture proportions of plain and D-GSH cement mortars.

Mixture	D-GSH	Dune Sand	Cement	Water	Dune Sand	D-GSH
	%	%	g/cm ³	g/cm ³	g/cm ³	g/cm ³ ($\times 10$)
Plain	0	100	0.865	0.432	0.865	0
M-G-0.3%	0.3	99.7	0.865	0.432	0.862	0.026

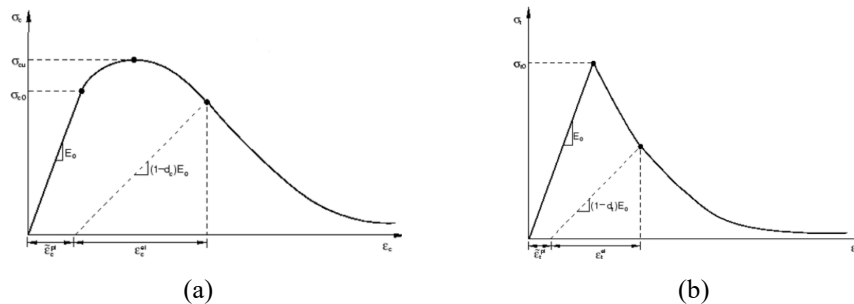


Fig. 1: Stress-strain models for cementitious composites: (a) Compressive and (b) Tensile responses

3. Finite Element Modelling

The FE model aimed to simulate a three-point load test of cement prisms, as per the setup described in ASTM C348 [15], through dynamic explicit analysis. ABAQUS offers three concrete material models, namely: the smeared crack model, the damaged plasticity model, and the cracking constitutive model. The concrete damage plasticity (CDP) model was considered in simulating the prismatic specimens subjected to flexure. The three-dimensional FE model of the prism had dimensions of 160×40×40-mm. A mesh size of 3 mm was considered for both FE models. A sensitivity analysis was conducted independently, considering different mesh sizes ranged between 1- and 7.5-mm, prior the selection of the mesh size. Figure 2(a-b) shows the modeled mortar prism subjected to a three-point load test.

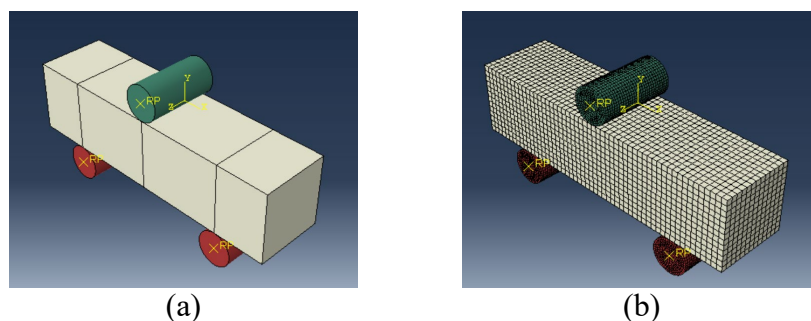


Fig. 2: 3D FE Model of three-point load Test of Mortar Prisms: (a) Model Parts, and (b) Model with a Mesh size of 3 mm

The total number of elements in meshing was 9126. The C3D8R eight-node continuum elements are based on the Lagrangian explanation of behavior where the elements deform together with the material deformation. A total of two boundary conditions were assigned which are: (1) the bottom steel rollers (acting as supports) were assigned as fixed (i.e., ENCASTE) with no displacement or rotation allowed, and (2) the top steel roller applying continuous load was allowed for vertical displacement only to simulate the described test. However, restricted displacements or rotations were enforced in any other directions to the top roller. The load applied in the vertical direction causing flexural behavior of the prismatic specimens was kept constant at 2.2 mm/sec.

4. Results & Discussion

Figure 3(a-b) presents the concentration of stresses in the plain and D-GSH-made cement mortar prism specimens subjected to flexural behavior. The mortar prism subjected to the flexure test had compression stresses at the interface with the supports and load application, while tension stresses were dominant at the bottom interface of the mid-span of the prism. Compared with the plain cement specimen, the addition of 0.3% D-GSH as a replacement of dune sand enhanced the Von Mises stresses by 20%, indicating an enhancement in flexural resistance.

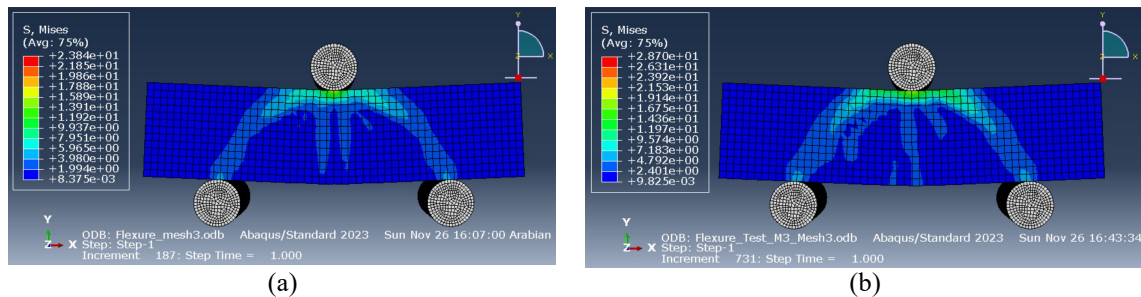


Fig. 3: Stress distribution within the FE models of (a) plain, and (b) M-G-0.3% prism specimens subjected to a three-point load test.

Figure 4 illustrates the load-deflection curves obtained from the three-point load tests conducted on mortar prism specimens. Both specimens exhibited a sudden fracture upon reaching the peak load, represented by the sudden drop in the load-deflection curves. The load-deflection response of the plain mortar showed a linear increase until reaching a peak load of 1.5 kN at a mid-span deflection of 0.31 mm. The specimen made with D-GSH had almost a similar linear increase in load except with a higher slope, representing a larger modulus of elasticity. The plain and D-GSH-made specimens resulted in flexural strengths of 4.2 and 5.3 MPa, respectively. Furthermore, the deflection at failure of the plain and D-GSH-made specimens was captured at 0.31- and 0.36-mm. The addition of 0.3% D-GSH, as a replacement for dune sand, enhanced flexural strength and mid-span deflection by at least 27% and 16%, respectively. These results indicate that the addition of only 0.3% D-GSH would enhance the overall flexural performance and deformability of the cement mortars.

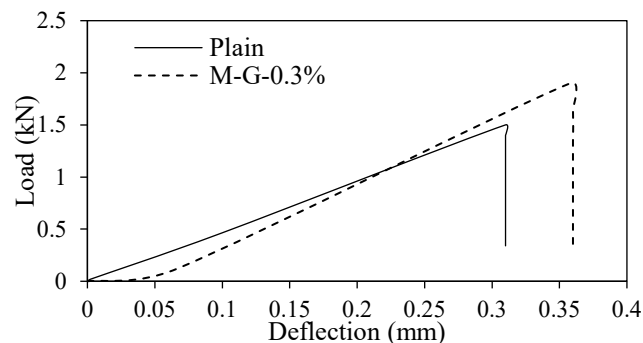


Fig. 4: Load-deflection curves of Plain and M-G-0.3% mortar prisms obtained from numerical modeling

5. Conclusion

In conclusion, this study employed a comprehensive approach, integrating experimental data and numerical to assess the influence of D-GSH addition on the flexural performance of cement mortars. The experimental results, through 28-day compressive strength and modulus of elasticity tests, served as crucial input for the ABAQUS finite model. The numerical simulations, considering both tensile cracking and compressive crushing mechanisms, revealed enhanced flexural resistance in D-GSH-modified mortars. The three-point bending tests further supported these findings, demonstrating a significant improvement in peak load and mid-span deflection with the addition of 0.3% D-GSH. This research underscores the potential of D-GSH as a sustainable additive, offering substantial enhancements in the flexural behavior and deformability of cement mortars with minimal dosage.

Acknowledgements

The authors would like to express their sincere appreciation to the Advanced Digital & Additive Manufacturing (ADAM) center at Khalifa University (No. 8474000163).

References

- [1] N. Makul, "Advanced smart concrete - A review of current progress, benefits and challenges," *J. Clean. Prod.*, vol. 274, p. 122899, Nov. 2020, doi: 10.1016/j.jclepro.2020.122899.
- [2] R. A. H. Ahmed Khalil and Mousa Attom, "Exploring Strength of Straight and Bent GFRP Bars: Refinements to CSA S807:19 Annex E," *ACI Symp. Publ.*, vol. 360, Mar. 2024, doi: 10.14359/51740628.
- [3] O. Mohamed and H. Zuaiter, "Fresh Properties, Strength, and Durability of Fiber-Reinforced Geopolymer and Conventional Concrete: A Review," *Polymers*, vol. 16, no. 1, p. 141, Jan. 2024, doi: 10.3390/polym16010141.
- [4] M. Zuaiter, H. El-Hassan, T. El-Maaddawy, and B. El-Ariss, "Performance of Hybrid Glass Fiber-Reinforced Slag-Fly ash Blended Geopolymer Concrete," presented at the The 8th International Conference on Civil, Structural and Transportation Engineering, Jun. 2023. doi: 10.11159/iccste23.113.
- [5] G. Goel, P. Sachdeva, A. K. Chaudhary, and Y. Singh, "The use of nanomaterials in concrete: A review," *Mater. Today Proc.*, vol. 69, pp. 365–371, 2022, doi: 10.1016/j.matpr.2022.09.051.
- [6] F. Y. Al-saffar, L. S. Wong, and S. C. Paul, "An Elucidative Review of the Nanomaterial Effect on the Durability and Calcium-Silicate-Hydrate (C-S-H) Gel Development of Concrete," *Gels*, vol. 9, no. 8, p. 613, Jul. 2023, doi: 10.3390/gels9080613.
- [7] S. Lv, H. Hu, J. Zhang, X. Luo, Y. Lei, and L. Sun, "Fabrication of GO/Cement Composites by Incorporation of Few-Layered GO Nanosheets and Characterization of Their Crystal/Chemical Structure and Properties," *Nanomaterials*, vol. 7, no. 12, p. 457, Dec. 2017, doi: 10.3390/nano7120457.
- [8] A. Gladwin Alex, A. Kadir, and T. Gebrehiwet Tewele, "Review on effects of graphene oxide on mechanical and microstructure of cement-based materials," *Constr. Build. Mater.*, vol. 360, p. 129609, Dec. 2022, doi: 10.1016/j.conbuildmat.2022.129609.
- [9] H. Yang, D. Zheng, W. Tang, X. Bao, and H. Cui, "Application of graphene and its derivatives in cementitious materials: An overview," *J. Build. Eng.*, vol. 65, p. 105721, Apr. 2023, doi: 10.1016/j.jobbe.2022.105721.
- [10] S. Khan, A. Achazhiyath Edathil, and F. Banat, "Sustainable synthesis of graphene-based adsorbent using date syrup," *Sci. Rep.*, vol. 9, no. 1, p. 18106, Dec. 2019, doi: 10.1038/s41598-019-54597-x.
- [11] ASTM, "C109/C109M: Standard Test Method for Compressive Strength of Hydraulic Cement Mortars." ASTM International, West Conshohocken, PA 19428-2959, United States.
- [12] ASTM, "C580-02: Standard Test Method for Flexural Strength and Modulus of Elasticity of Chemical Resistant Mortars, Grouts, Monolithic Surfacing, and Polymer Concretes1." ASTM International, West Conshohocken, PA 19428-2959, United States., 2008.
- [13] A. Khalil, M. Elkafrawy, R. Hawileh, M. AlHamaydeh, and W. Abuzaid, "Numerical Investigation of Flexural Behavior of Reinforced Concrete (RC) T-Beams Strengthened with Pre-Stressed Iron-Based (FeMnSiCrNi) Shape Memory Alloy Bars," *J. Compos. Sci.*, vol. 7, no. 6, p. 258, Jun. 2023, doi: 10.3390/jcs7060258.

- [14] Y. Tan, Q. Gu, J. Ning, X. Liu, Z. Jia, and D. Huang, “Uniaxial Compression Behavior of Cement Mortar and Its Damage-Constitutive Model Based on Energy Theory,” *Materials*, vol. 12, no. 8, p. 1309, Apr. 2019, doi: 10.3390/ma12081309.
- [15] ASTM, “C348–08: Standard Test Method for Flexural Strength of Hydraulic-Cement Mortars.” ASTM International, West Conshohocken, PA 19428-2959, United States.
- [16] Khalil, A.M., Hawileh, R. and Attom, M., 2024. “Investigating the Durability of Bent and Straight Glass Fiber Reinforced Polymer (GFRP) Rebars: Pilot Study”. In 9th International Conference on Civil, Structural and Transportation Engineering, ICCSTE 2024. Avestia Publishing